THE 1996 SOFT STATE TRANSITION OF CYGNUS X-1

S. N. ZHANG,[1, 2] W. CUI,[3] B. A. HARMON,[1] W. S. PACIESAS,[1, 4] R. E. REMILLARD,[3] AND J. VAN PARADIJS[4, 5]

ABSTRACT

We report continuous monitoring of Cygnus X-1 in the 1.3–200 keV band using All-Sky Monitor/*Rossi X-Ray Timing Explorer* and BATSE/*Compton Gamma Ray Observatory* for about 200 days from 1996 February 21 to early September. During this period, Cygnus X-1 experienced a hard-to-soft and then a soft-to-hard state transition. The low-energy X-ray (1.3–12 keV) and high-energy X-ray (20–200 keV) fluxes are strongly anticorrelated during this period. During the state transitions, flux variations of about a factor of 5 and 15 were seen in the 1.3–3.0 keV and 100–200 keV bands, respectively, while the average 4.8–12 keV flux remains almost unchanged. The net effect of this pivoting is that the total 1.3–200 keV luminosity remained unchanged to within ∼15%. The bolometric luminosity in the soft state may be as high as 50%–70% above the hard state luminosity, after color corrections for the luminosity below 1.3 keV. The blackbody component flux and temperature increase in the soft state are probably caused by a combination of the optically thick disk mass accretion rate increase and a decrease of the inner disk radius.

Subject headings: accretion, accretion disks — black hole physics — stars: individual (Cygnus X-1) —
X-rays: stars

1. INTRODUCTION

Cygnus X-1 is one of the brightest high-energy sources in the sky, with an average 1–200 keV energy flux of ∼3×10^{-8} ergs cm^{-2} s^{-1}. Most of the time, its X-ray spectrum is very hard, with a high-energy (>20 keV) X-ray flux around or above that of the Crab Nebula, while its low-energy (<10 keV) X-ray flux is around 0.5 Crab. Occasionally, the spectrum of Cyg X-1 becomes much softer; then its low-energy X-ray flux increases to 1–2 Crab, while the hard X-ray flux decreases to 0.5 Crab or less. On the basis of the radial velocity curve of its O9.7 Iab companion star, Webster & Murdin (1972) and Bolton (1972) concluded that the compact star in Cyg X-1 may be a black hole (BH); their results have been confirmed by later detailed work of Gies & Bolton (1986), who concluded that the mass of the compact object in Cyg X-1 is greater than 7 $M_\odot$, but more probably 16 $M_\odot$, far exceeding the theoretical (and observational) upper mass limit of 3.2 $M_\odot$ for a neutron star. It is thus the first stellar mass BH candidate (BHC) (cf. Liang & Nolan 1984 and Tanaka & Lewin 1995, for reviews and references therein).

Cyg X-1 is often considered as the canonical BHC; many of its characteristics, such as its high X-ray luminosity above 100 keV, the ultrasoft component in its X-ray spectrum, the hard/soft X-ray flux anticorrelation, and the rapid X-ray flux variability, are shared by other systems, which, on the basis of a dynamical mass estimate, may contain a BH. However, it is not understood currently why accreting BHs show these characteristics.

In spite of extensive studies over the last three decades, the mass accretion conditions near the central compact object in Cyg X-1 and other BH systems, and the high-energy radiation mechanism, are still poorly understood. This remains an

outstanding issue in high-energy astrophysics. State transitions fully covered over a large range in X-ray photon energy may provide us with important clues toward a better understanding of these BH X-ray binaries. During a transition, a rich collection of information may be obtained, such as flux variations at many timescales in all energy bands, energy spectral evolution, correlations between different energy bands, etc.; such data should provide useful tests of various theories and models.

Previously, several transitions between the hard state (HS) and the soft state (SS) of Cyg X-1 have been observed. In 1971, a soft-to-hard (S-to-H) state transition was observed in the 2–20 keV band (Tananbaum et al. 1972). In 1975, a complete transition was observed with *Ariel 5* between 3 and 6 keV (Holt et al. 1976), and by *Vela* between 3 and 12 keV (Priedhorsky, Terrell, & Holt 1983). These observations were limited to rather low X-ray energies. The only broadband observations of a transition were obtained in 1980, with *Hakucho* between 1 and 12 keV (Ogawara et al. 1982) and with *HEAO 3* between 48 and 183 keV (Ling et al. 1983). However, the SS onset was observed only with *HEAO 3* as a rapid decrease in the 48–183 keV flux, and then later the SS was observed with *Hakucho* only when the 1–12 keV flux was already a factor of 2–3 higher than its HS level before the transition. Therefore, no simultaneous, low- and high-energy X-ray observations during S-to-H or hard-to-soft (H-to-S) transitions of Cyg X-1, have been made so far.

In this Letter, we report results obtained from the near continuous monitoring of Cyg X-1 during a complete state transition from the HS to the SS (Cui 1996; Cui, Focke, & Swank 1996; Zhang et al. 1996b), and then back to the HS (Zhang, Harmon, & Paciesas 1996a; Zhang et al. 1996c), observed simultaneously with the ASM/*RXTE* (1.3–12 keV) and the BATSE/*CGRO* (20–200 keV) for about 200 days from 1996 February to September. Our results are complemented by detailed pointing observations with the *Advanced Satellite for Cosmology and Astrophysics* (*ASCA*) (0.5–10 keV) (Dotani et al. 1996), with the PCA and HEXTE (2–250 keV) aboard *RXTE* (Cui et al. 1996, 1997; Belloni et al. 1996), with

[1] ES-84, NASA/Marshall Space Flight Center, Huntsville, AL 35812.

[2] Universities Space Research Association.

[3] Center for Space Research, Massachusetts Institute of Technology, Cambridge, MA 02139.

[4] University of Alabama in Huntsville, Huntsville, AL 35899.

[5] University of Amsterdam, Sterrenkundig Instituut "Anton Pannekoek," Kruislaan 403, 1098 SJ Amsterdam.
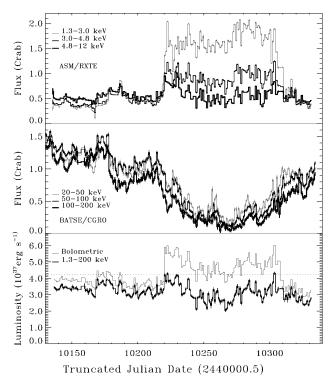
FIG. 1.—Cyg X-1 light curves and the 1.3–200 keV luminosity variations during its 1996 SS transition.

the SAX (0.1–300 keV) (Piro et al. 1996), and with the OSSE/*CGRO* (50–600 keV) (Phlips et al. 1997). We will focus on variations in the total luminosity during this period and on the correlations between the low-energy and high-energy X-ray fluxes.

2. OBSERVATIONAL DATA

The *Rossi X-Ray Timing Explorer* (*RXTE*) was launched on 1995 December 30. The All-Sky Monitor (ASM) began normal operation on 1996 February 21. More than 70 sources have been monitored routinely in three energy bands (1.3–3.0, 3.0–4.8, and 4.8–12 keV). A detailed description of the performance of the ASM, as well as its calibration and data reduction procedures, has been given by Levine et al. (1996).

The BATSE experiment is one of the four instruments aboard the *Compton Gamma Ray Observatory* (*CGRO*) and has operated continuously since launch in 1991 April. BATSE can monitor the entire hard X-ray (HXR) sky with almost uniform sensitivity for the detection of gamma-ray bursts, solar flares, pulsars. and other persistent and transient HXR sources (Fishman et al. 1989). The persistent and transient HXR source monitoring is achieved by using the Earth occultation technique (Harmon et al. 1992) and the Earth occultation transform imaging technique (Zhang et al. 1993). Cyg X-1 has been one of the brightest sources in the BATSE database, in which it is detected from 20 to above 300 keV (see Crary et al. 1996 and Paciesas et al. 1996 for recent papers describing results of analyses of the BATSE data on Cyg X-1).

3. LIGHT CURVES AND TOTAL LUMINOSITY VARIATIONS

The daily averaged ASM light curves in the three energy bands are plotted in Figure 1 (*upper panel*), in units of the total Crab Nebula counting rates detected by ASM in the same

energy bins. The three-channel data on each day would overlap each other for an energy spectrum with the same shape as that of the Crab Nebula (power law with a photon index of ~-2). For a steeper spectrum, the lower energy channel data will lie above the higher energy data and vice versa. In the middle panel of the figure, we plot the three energy band (20–50, 50–100, and 100–200 keV) BATSE light curves. There are a total of 8–9 energy channels covering the 20–200 keV energy range. For each energy band, we use the detector response matrices and integrate over the relevant energy channels to produce the photon fluxes, by assuming a power-law shape of a photon index of -2.0. The fluxes are then divided by the fluxes of the Crab Nebula detected with BATSE in the same energy range. By converting the fluxes to "Crab" units, we avoid possible absolute detector calibration problems between ASM and BATSE.

Two spectral state transitions occurred near TJD 10220 and TJD 10307, characterized by the rapid increase and decrease of the ASM low-energy flux. We call the state "hard state" before TJD 10220 and after TJD 10307, since the overall spectral shape is harder than that of the Crab Nebula. Similarly, we call the state between the transitions the "soft state." The HS spectrum is characterized by a hard power law between 1.3 and 100 keV, with a photon index of around -1.8. The 20–50 keV flux is above the power law by 20%–30%. Above 100 keV, a spectral cutoff is observed. In the SS, the overall 3–200 keV spectrum is dominated by a power law with a photon index of about -2.5. The first ASM energy band is contaminated significantly by a soft excess. A flux excess between 20 and 50 keV above the power law, similar to the HS spectrum, makes the overall 20–200 keV spectrum fit reasonably well with a cutoff power-law model. The details of the spectral evolution will be presented elsewhere (Zhang et al. 1997).

In the bottom panel of the figure, we plot the total luminosity observed with ASM and BATSE between 1.3 and 200 keV. For the ASM bands, the luminosity is calculated in each band separately by assuming the Crab Nebula spectrum shape. A hydrogen column density $N_H \sim 5.5 \times 10^{21}$ atoms cm^{-2} (Ebisawa et al. 1996) is used for correcting the absorption in the 1.3–3.0 band. This correction is not sensitive to the exact value of N_H we used. The luminosity would be underestimated in the 1.3–3.0 keV only by $\sim5\%$ if the true N_H is 7.0×10^{21} atoms cm^{-2}. The luminosity in the BATSE energy range (20–200 keV) is calculated by assuming that the energy spectrum is a power law with an exponential cutoff (e.g., Sunyaev & Truemper 1979; Sunyaev & Titarchuk 1980) (the power-law index and the cutoff energy on each day were separately determined from spectral fits to the daily averaged count rates in eight or nine spectral energy bands). The gap between the ASM and the BATSE energy bands is filled by interpolating the 4.8–12 keV and the 20–30 keV fluxes and assuming again a power-law energy spectrum. Overall, we estimate that the deviations of the calculated luminosity should be less than 10% of the true luminosity in the 1.3–200 keV energy band. A distance of 2.5 kpc is assumed for Cyg X-1 in these calculations.

There is a general anticorrelation between the ASM fluxes and the BATSE fluxes. The fractional rms variations, calculated from the daily averaged fluxes, in the six energy bands are 62% (1.3–3.0 keV), 40% (3.0–4.8 keV), 17% (4.8–12 keV), 43% (20–50 keV), 54% (50–100 keV), and 62% (100–200 keV). As a comparison, the 1.3–200 keV luminosity rms

fractional variation is about 15%. This behavior indicates a spectral pivoting at around 10 keV.

To obtain the bolometric luminosity, we need to correct for the flux emitted beyond both the low-energy (1.3 keV) and the high-energy (200 keV) limits of our observations. The high-energy correction is not important because of the rather steep spectral cutoff around 100 keV in the HS and the rather steep power law (photon index around -2.5) in the SS. The total luminosity above 200 keV is comparable in both the HS and the SS, and amounts to less than 10% of the bolometric luminosity.

The low-energy cutoff correction is necessary because a significant portion of the ultrasoft component is not detected with ASM. This component can be fitted with a blackbody (BB). For the HS, values of $kT_{bb} \sim 0.12$–0.16 keV were obtained from one *ROSAT* (0.1–2.0 keV) observation on 1991 April 18–20 (Balucinska-Church et al. 1995) and 10 *ASCA* (0.5–10 keV) observations between 1993 October and 1994 December (Ebisawa et al. 1996). Values of $kT_{bb} \sim 0.34$ keV were obtained in the SS, obtained from one *ASCA* observation on 1996 May 30 during the SS (Dotani et al. 1996), and from 11 *RXTE* PCA and HEXTE observations throughout the whole SS (Cui et al. 1996). The *RXTE* data indicate that the BB temperature is slightly higher in some *RXTE* observations (Cui et al. 1996). We thus take the 0.34 keV as the lower limit of the BB temperature in the SS. It is not possible to estimate the BB component in the HS from the ASM data since the power-law component dominates the ASM HS detector counting rates. Previous *ROSAT* and *ASCA* observations of Cyg X-1 in the HS revealed a BB component luminosity level of about 5×10^{36} ergs s^{-1}. We added this value to the HS 1.3–200 keV luminosity, as shown in the bottom panel of Figure 1. The soft excess accounts for about 50%–70% of the 1.3–3.0 keV ASM counts in the SS. Taking the BB temperature $kT \gtrsim 0.34$ keV, we estimate that the BB luminosity below 1.3 keV is $\lesssim (1.2$–$1.7) \times 10^{37}$ ergs s^{-1} [the total SS BB luminosity is $\lesssim (2.2$–$3.1) \times 10^{37}$ ergs s^{-1}]. The value of 1.7×10^{37} ergs s^{-1} is added to the SS 1.3–200 keV luminosity, as depicted in the bottom panel of Figure 1. In summary, SS bolometric luminosity is between the thin curve and the thick curve.

The bolometric luminosity displays an increase and decrease by $\lesssim 50$%–70% during the H-to-S and S-to-H state transitions. In the middle of the SS, however, the luminosity is only $\lesssim 10$%–20% higher than the HS luminosity, because of the gradual decrease of the HXR flux after the initial SS transition and the almost symmetric recovery after reaching the minimum HXR flux between TJD 10260 and 10275, while the soft excess in the 1.3–3.0 keV band, averaged over several days, stayed at about 1.5 Crab during the entire SS. Therefore, the bolometric luminosity variations throughout the state transitions are less than 50%–70%.

4. DISCUSSION

Compared with the high-energy observations of the previous Cyg X-1 SS transitions, the data presented here are the first set covering the whole transition episode continuously over a broad energy band. The observed 1.3–15 keV (*Ariel 5*) spectral evolution (spectral pivoting and power-law index changes) (Chiappetti et al. 1981) during the 1975 S-to-H state transition is quite similar to that presented here. The initial HXR flux and spectral steepening observed with *HEAO 3* between 48 and 183 keV (Ling et al. 1983), and the soft X-ray flux level

between 1 and 12 keV observed later with *Hakucho* (Ogawara et al. 1982), are similar to that during the SS presented here. Both previous SSs lasted between 60 and 100 days, again similar to the 1996 SS duration. So this 1996 SS transition is qualitatively similar to the previous ones. It is thus reasonable to assume that the same physical mechanism is responsible for all of them.

GX 339-4 is the only other BHC observed to have recurrent state transitions. From a comparison with its 1981 H-to-S state transition (Maejima et al. 1984), we find that the HS spectra of this source and Cyg X-1 are quite similar. The ratio between the SS and the HS total luminosity observed from GX 339-4 (e.g., Ricketts 1983) is also similar to that of Cyg X-1 presented here. During a SS observation of GX 339-4 in 1983 (Makishima et al. 1986), the HXR flux increased significantly, while the soft X-ray flux remained nearly unchanged, also similar to the HXR flux increase in the second half of the SS of Cyg X-1. The photon index of the power law changed from -0.9 to -2.1 following the HXR flux increase of GX 339-4, different from the near constant value of -2.5 during much of the SS in Cyg X-1. However, the power-law tail during a "very high" state of GX 339-4 (Miyamoto et al. 1991), when the overall flux was about a factor of 2–3 higher than during the previous SS observations, is very similar to that of Cyg X-1 in the SS. Qualitatively similar S-to-H state transitions have also been observed from the low-mass X-ray binary BH system GS 1124-683 (Ebisawa et al. 1994) and the neutron star system 4U 1608-52 (Mitsuda et al. 1989). Therefore, similar physical mechanisms might operate in all of them.

The "hard" and "soft" states we refer to in this Letter are usually called the "low" and "high" (and "very high") states. This is due to the fact that the early observations of them were made in the low-energy X-ray band (<20 keV; see, e.g., Tananbaum et al. 1972), so the terms "low" and "high" refer to the low and high values of the low-energy X-ray fluxes, respectively. It is generally believed that the low-energy X-ray flux tracks the total mass accretion rate of the system; therefore, these "low" and "high" states have been considered to correspond to low and high values of $\dot{M}$, respectively. This idea gained strong support in the unified scheme of source states of both neutron star and BH X-ray binaries proposed by van der Klis (1995).

This picture may be incomplete in view of the lack of a strong variation of the total luminosity during the state transitions that we observed in 1996. The blackbody component detected in both hard and soft states is generally thought to originate from an optically thick and geometrically thin accretion disk near the BH (see, e.g., Mitsuda et al. 1984). According to current models, the hard power-law spectral component is likely produced in a very hot and optically thin region, through Comptonization of low-energy X-ray photons; the detailed nature of the optically thin region and the mechanism that makes it very hot distinguish these different models. The near constant luminosity during the transitions indicates that they are driven by a redistribution of the gravitational energy release between the optically thick and the optically thin regions. Therefore, *a H-to-S state transition, and its reverse, probably reflects a change in the relative importance of the energy release in the optically thin and thick regions of the accretion disk near the BH, and this may not require a substantial change in the total accretion rate.*

Spectra emitted by accretion disks around black holes are well described by the "multitemperature disk blackbody

model" of Mitsuda et al. (1984), which has as fit parameters the inner disk radius, R_{in}, and the temperature, T_{in}, at that radius. It is usually assumed that the inner disk radius equals 3 times the Schwarzschild radius, and this provides acceptable mass estimates for the black hole (see Tanaka & Lewin 1995 for a review).

The blackbody fits made to the high-energy tail of this multitemperature disk BB model provide good fits for a blackbody temperature, T_{bb}, which turns out to be equal to the temperature in the disk at a radius of about 7 Schwarzschild radii (Ross, Fabian, & Mineshige 1992); correspondingly, one has $T_{bb} \simeq 0.7 T_{in}$. Independent of the ratio of inner disk radius to the Schwarzschild radius, one has $T_{bb} \propto T_{in}$. Since, in the multitemperature disk model, the bolometric luminosity ($L_{bol,disk}$), follows the proportionality relation $L_{bol,disk} \propto R_{in}^2 T_{in}^4$, one has $(L_h/L_s) = (R_h/R_s)^2(T_h/T_s)^4$, by applying the proportionality relation in both the HS and the SS, where the subscripts h and s denote the hard state and the soft state, respectively.

From the observations, we infer that $L_s/L_h \lesssim 6$, and $T_s/T_h \gtrsim$ 2.1–2.8. Consequently, we obtain $R_h/R_s \gtrsim$ 1.8–3.2. This result suggests that *during the H-to-S transition, the inner radius of the geometrically thin and optically thick disk changed from $\gtrsim 170$ to ~ 70 km* (the latter value has been obtained by Dotani et al. 1997, from *ASCA* observations during the soft state). Applying the relationship between the mass accretion rate, the inner disk radius, and the inner disk temperature in the multitemperature disk model, we have $\dot{M}_s/\dot{M}_h \lesssim$ 2.0–3.4.

This change in inner disk radius accompanying the spectral state changes suggests a picture in which, during the hard state, advection of internal disk energy into the black hole, as proposed by Narayan (1996), dominates within a radial distance of $\gtrsim 170$ km from the hole. In the soft state, the flow in the inner disk may still be advection-dominated, with only a moderate fraction of the mass flow passing through an optically thick inner disk.

Variations of the inner disk radius have also been discussed

by Ebisawa et al. (1996), in the context of the mass accretion and high-energy radiation model of Chakrabarti & Titarchuk (1995), and have recently been proposed by Belloni et al. (1996) as an explanation for the rapid variability of the black hole candidate GRS 1915 + 105 (albeit at much higher mass accretion rates).

A potential problem for any model that purports to explain the spectral transitions in terms of an instability in the inner disk region is that the transitions seem to be accompanied by the gradual changes in the slope and the flux of the HXR power-law component, which occur over a very long timescale (approximately weeks). In fact, the 1996 S-to-H transition was predicted from the HXR flux increase (Zhang et al. 1996c). It is possible that Cyg X-1 underwent a very slow change in the mass accretion rate, which initially only affected the properties of the hard X-ray emission region. The sudden soft (1.3–3.0 keV) X-ray flux increase and decrease over a much shorter timescale, during the state transitions, may then represent the crossing of a threshold, at which the radiative efficiency exceeds a value required for the formation of an optically thick disk down to the innermost stable orbit.

In view of the observational limitations, the above remarks are necessarily somewhat speculative. It would appear that a better understanding of the cause of the spectral state changes in Cyg X-1 requires that further monitoring of the long-term behavior of Cyg X-1 include low-energy (≤ 1 keV) coverage of the source as well.

REFERENCES

Balucinska-Church, M., Belloni, T., Church, M. J., & Hasinger, G. 1995, A&A, 302, L5
Belloni, T., Méndez, M., van der Klis, M., Hasinger, G., Lewin, W. H. G., & van Paradijs, J. 1996, ApJ, 472, L107
Bolton, C. T. 1972, Nature, 235, 271
Chakrabarti, S. K., & Titarchuk, L. 1995, ApJ, 455, 623
Chiappetti, L., Blissett, R. J., Branduardi-Raymont, G., Bell Burnell, S. J., Ives, J. C., Parmar, A. N., & Sanford, P. W. 1981, MNRAS, 197, 139
Crary, D. J., et al. 1996, ApJ, 462, L71
Cui, W. 1996, IAU Circ. 6404
Cui, W., Focke, W., & Swank, J. 1996, IAU Circ. 6439
Cui, W., Heindl, W. A., Rothschild, R. E., Zhang, S. N., Jahoda, K., & Focke, W. 1997, ApJ, 474, L57
Dotani, T., Negoro, H., Mitsuda, K., Inoue, H., & Nagase, F. 1996, IAU Circ. 6415
Dotani, T., et al. 1997, PASJ, submitted
Ebisawa, K., et al. 1994, PASJ, 46, 375
Ebisawa, K., Ueda, Y., Inoue, H., Tanaka, Y., & White, N. E. 1996, ApJ, 467, 419
Fishman, G. J., et al. 1989, in *Gamma Ray Observatory Science Workshop*, ed. C. R. Shrader, N. Gehrels, & B. Dennis (CP-3137; Greenbelt: NASA) 2-39
Gies, D. R., & Bolton, C. T. 1986, ApJ, 304, 371
Harmon, B. A., et al. 1992, in AIP Conf. Proc. 280, *Compton Gamma Ray Observatory* (New York: AIP), 314
Holt, S. S., et al. 1976, ApJ, 203, L63
Levine, A. M., Bradt, H., Cui, W., Jernigan, J. G., Morgan, E. H., Remillard, R., Shirley, R. E., & Smith, D. A. 1996, ApJ 469, L33
Liang, E. P., & Nolan, P. L. 1984, Space Sci. Rev., 38, 353
Ling, J. C., Mahoney, W. A., Wheaton, W. A., & Jacobson, A. S. 1983, ApJ, 275, 307
Maejima, Y., Makishima, K., Matsuoka, M., Ogawara, Y., Oda, M., Tawara, Y., & Doi, K. 1984, ApJ, 285, 712

Makishima, K., Maejima, Y., Mitsuda, K., Bradt, H. V., Remillard, R. A., Tuohy, I. R., Hoshi, R., & Nakagawa, M. 1986, ApJ, 308, 635
Miyamoto, S., Kimura, K., Kitamoto, S., Dotani, T., & Ebisawa, K. 1991, ApJ, 383, 784
Mitsuda, K., et al. 1984, PASJ, 36, 741
Mitsuda, K., Inoue, H., Nakamura, N., & Tanaka, Y. 1989, PASJ, 41, 97
Narayan, R. 1996, ApJ, 462, 136
Ogawara, Y., Mitsuda, K., Masai, K., Vallerga, J. V., Cominsky, L. R., Grunsfeld, J. M., Kruper, J. S., & Ricker, G. R. 1982, Nature, 295, 675
Paciesas, W. S., et al. 1996, 31st COSPAR Scientific Assembly, Birmingham, UK
Phlips, B., et al. 1997, in preparation
Piro, L., et al. 1996, IAU Circ. 6431
Priedhorsky, W. C., Terrell, J., & Holt, S. S. 1983, ApJ, 270, 233
Ricketts, M. 1983, A&A, 118, L3
Ross, R. R., Fabian, A. C., & Mineshige, S. 1992, MNRAS, 258, 189
Sunyaev, R., & Titarchuk, L. 1980, A&A, 86, 121
Sunyaev, R., & Truemper, J. 1979, Nature, 279, 506
Tanaka, Y., & Lewin, W. H. G. 1995, in X-Ray Binaries, ed. W. H. G. Lewin, J. van Paradijs, & E. P. J. van den Heuvel (Cambridge: Cambridge Univ. Press), 126
Tananbaum, H., et al. 1972, ApJ, 177, L4
van der Klis, M. 1995, in X-Ray Binaries, ed. W. H. G. Lewin, J. van Paradijs, & E. P. J. van den Heuvel (Cambridge: Cambridge Univ. Press), 126
Webster, B. L., & Murdin, P. 1972, Nature, 235, 37
Zhang, S. N., Fishman, G. J., Harmon, B. A., & Paciesas, W. S. 1993, Nature, 366, 245
Zhang, S. N., Harmon, B. A., & Paciesas, W. S. 1996a, IAU Circ. 6447
Zhang, S. N., Harmon, B. A., Paciesas, W. S., & Fishman, G. J. 1996b, IAU Circ. 6405
Zhang, S. N., et al. 1996c, IAU Circ. 6462
Zhang, S. N., et al. 1997, ApJ, in press